2020 IEEE International Conference on Robotics and Automation (ICRA)
31 May - 31 August, 2020. Paris, France

A Robotics Inspection System for Detecting Defects on Semi-specular Painted Automotive Surfaces

Sohail Akhtar[1], Adarsh Tandiya[2], Medhat Moussa[1], Cole Tarry[1]

Abstract— **This paper describes the design and implementation of a real-time robotics system for semi-specular/painted surface defect detection. The system can be used on moving parts, tolerate varying lighting conditions, and can accommodate small inherent vibrations of the inspected surface that is common in manufacturing operations. Topographical information of the inspected surface is first obtained by the analysis of reflections of a known pattern from this surface. Spectral analysis is then applied to identify defects through novelty detection. Finally, a defect tracking mechanism eliminates spurious defects. The proposed system operates continuously at 90 fps. The paper presents field testing results that show the system can be used as a consistent and cost-effective way of quality control.**

I. Introduction

Vision-based surface inspection systems are used for online detection of defects on different sucfaces such as aluminium strips [1], rail surfaces [2], plastic surfaces [3], sphere parts [4], food products [5], and textile fabric [6].

The focus of this paper is on the inspection of large, painted automobile exterior body parts like bumpers and facia. It is important to have zero defects on these parts as it makes the first impression for a car buyer. At present, the inspection task is mostly carried out by human inspectors whose performance is generally subjective, variable, time-consuming and prone to errors. Automated inspection of these parts surfaces is challenging due to several reasons. Parts have different shapes, sizes, curvatures, colour, and surfaces that are semi-specular with different reflection coefficients [1]. Occurring defects have different shapes and sizes, and there are no fixed criteria for inspection, which results in inconsistencies between human inspectors. Finally, the inspection process must be completed while parts are in motion through the production line mounted on specialized carriers that are mildly vibrating.

Interferometry and Deflectometry are two methods used for automatic inspection for these parts. The use of interferometry is limited in industrial applications due to the requirement for compensation optics, slower system calibration. It is susceptible to coherent noises when subjected to harsh temperature and pressure [7]. On the other hand, Deflectometry is currently used for this task [8]. It exploits the reflective characteristics of specular/semi-specular surfaces. A known pattern is displayed on an LCD screen directed to the test surface. The surface reflections of the pattern are then captured by a camera and analyzed for 3-D surface reconstruction. Phase-Shift Deflectometry (PSD) in particular is a popular method of surface defect detection [9]–[16]. This method requires at least three fringes (usually 5-7 patterns are used for reliable defect detection [11], [16]). The surface needs to be stationary during the capturing process. As such, the inspection process is relatively slow and can't be carried out while the parts are moving or vibrating. Still, there are reports of deflectometry based systems that are deployed commercially. Armesto et al. [9] described a system deployed at Ford Motor plant. It uses a moving structure consisting of light bars and several fixed position cameras around a stationary car body. Similarly, Molina et al. [17] describe a system deployed at a Mercedes-Benz factory in Victoria, Spain. This system completes its inspection in 30 seconds and requires a stationary car body. Akhtar et al. [18], proposed a deflectometry based system to inspect small painted parts inspection system at a stationary station. Other inspection systems used different techniques. Fan et al. [19] uses an indirect diffusion light system that applies both pattern-light and full-light. It uses frequency analysis as well as defect size assumptions to detect defects. Zhou et al. [20] presented a system for defect detection that uses a multi-scale Hessian matrix fusion method for extracting defect candidates. These defects are later classified into dents, scratches and pseudo-defects.

All of the reviewed previous methods for detecting defects on semi-specular car body parts require stationary objects which require significant modifications to production cycle time.

A. Main Contributions

In this paper, we present a new automotive paint defect detection system. This system uses Phase-only-transform (PHOT) technique, which requires a single image for defect detection rather than multiple images that are normally required for Phase-shift deflectometry. As a result, it can be used on a continuous running assembly line. Phase-only-transform (PHOT) was initially used for fabric defect detection [30]. However, using PHOT for defect detection on specular surface while in motion is very challenging for several reasons. Solving these challenges is the main contribution of this paper.

- To enable inspection of parts while in motion, the system is mounted on a robot end-effector that traverses the part surface and captures surface reflections in the form of a continuous video. The robot tracks the part's

[1]Sohail Akhtar, Medhat Moussa, Cole Tarry are with School of Engineering, University of Guelph, Guelph, Canada, [2]Adarsh Tandiya is with Praemo Inc., Kitchener, Canada, soakhtar, atandiya, mmoussa, ctarry@uoguelph.ca

movement and thus does not require the part to be stationary.
- A novel defect tracking algorithm is implemented to eliminate false defects due to any noise registered during the image capturing process or due to acute surface changes.
- The PHOT algorithm is modified by adding horizontal and vertical 1-D Fourier transform to overcome the PHOT difficulty in detecting line-shaped defects due to the inherent characteristic of the Fourier transform [30].

The remainder of this paper is organized as follows. Section 2 describes the working principle of the proposed system. Section 3 provides details on the defect detection system and its various components. Section 4 describes the experimental setup and presents results with detailed analysis. Finally, Section V summarizes the findings of this research and highlights some areas of future development.

II. Working Principle

The Phase-only-transform (PHOT) technique [30] exploits the phase of a signal which carries high-frequency edge information for abnormality detection. This method does not require any prior information or learning. This phase information is transformed back to the spatial domain for defect localization.

Phase only transform

The two dimensional DFT of an image is defined by Equation 1 [33]:

$$\mathcal{F}(u,v) = \frac{1}{MN} \sum_{x=0}^{M-1} \sum_{y=0}^{N-1} I(x,y)\, e^{-j\, 2\pi (\frac{u}{M} x + \frac{v}{N} y)} \quad (1)$$

where $j = \sqrt{-1}$, the indices(u, v) are the spatial frequencies of transformation, $I(x, y)$ is the image intensity at spatial location (x, y), M and N are the width and the height of the image and $\mathcal{F}(u, v)$ is the resultant complex transform which can also be represented as a complex number:

$$\mathcal{F}(u,v) = \mathcal{R}(u,v) + j\,\mathcal{I}(u,v) \quad (2)$$

where $\mathcal{R}(u, v)$ and $\mathcal{I}(u, v)$ are real and imaginary parts of the resultant transform. In polar form the transform can be represented as:

$$\mathcal{F}(u,v) = \mathcal{M}(u,v)\, e^{-j\,\phi(u,v)} \quad (3)$$

where $\mathcal{M}(u, v)$ is magnitude and $\phi(u, v)$ is the phase variations and are defined as:

$$\mathcal{M}(u,v) = \sqrt{\mathcal{R}^2(u,v) + \mathcal{I}^2(u,v)} \quad (4)$$

$$\phi(u,v) = tan^{-1}\left[\frac{\mathcal{I}(u,v)}{\mathcal{R}(u,v)}\right] \quad (5)$$

Dividing Equation 2 by the magnitude $\mathcal{M}(u, v)$ and taking the inverse DFT will result in a phase-only-image. The effect of dividing the DFT by magnitude is that the regular pattern's phase value is diminished as it is divided by a larger magnitude due to the periodic occurrence of the pattern and hence will be removed in the phase-only-image. On the other hand, the phase value of rare events is accentuated as they are divided by a smaller magnitude and will be amplified in phase-only-image. As a result, all the background information will be removed.

The PHOT algorithm is robust over varying illumination conditions and different background image patterns. Its execution is also fast as the complexity of the algorithm is in the order of $O(nlogn)$, where n is the number of pixels in the image.

III. Defect Detection System Design

The proposed defect detection system consists of several components starting from reflected pattern generation and ends at defect attributes registration, as depicted in Fig. 1. A pattern is displayed on a monitor that is projected on the test surface. The attached camera captures the reflection from the test surface. Since the inspected parts are large and of complex geometry, so they cannot be inspected in a single image. Hence, the screen camera setup is attached to a robot end-effector which traverses the inspected part as it moves while maintaining a fixed distance between the camera and test part and collects the surface profile in the form of a continuous stream of images. This setup is depicted in Fig. 2. The different components of the defect detection system are detailed in the following sections:

A. Image capture

The camera is attached to the pattern screen side so that it captures the centre of the projected pattern on the test surface, as shown in Fig. 3. A solid white pattern is used as the illumination source. The camera captures the reflection of this white pattern from the test surface. The reflected pattern is distorted in the captured image. This distortion is due to the irregular reflection of light from the surface. The irregularities reflect defects in the test surface and hence appears differently in the image. These surface attributes are collected as the robot scans the test part.

B. Pre-processing and defect detection

A Gaussian kernel smoothens the captured image for noise removal. A fixed focus camera is used, which captures a fixed size image that contains both the pattern projected region and the non-pattern region. Since the size of the reflected pattern varies with the surface curvature, the pattern appears to shrink if the surface is convex and vice versa. Hence, the system starts with a segmentation step where only the projected pattern is extracted as the region of interest (ROI). After this initial pre-processing step, the 2D FFT is applied to the image and the resultant complex transform is divided by the magnitude of the spectrum. This step will suppress all the background information from the signal, i.e., regular patterns in the image are eliminated. Later on, inverse FFT is computed to obtain the background suppressed image, called PHOT image. This image is smoothened by a Gaussian kernel and then Mahalanobis distance is computed by subtracting the mean PHOT image pixel intensity from

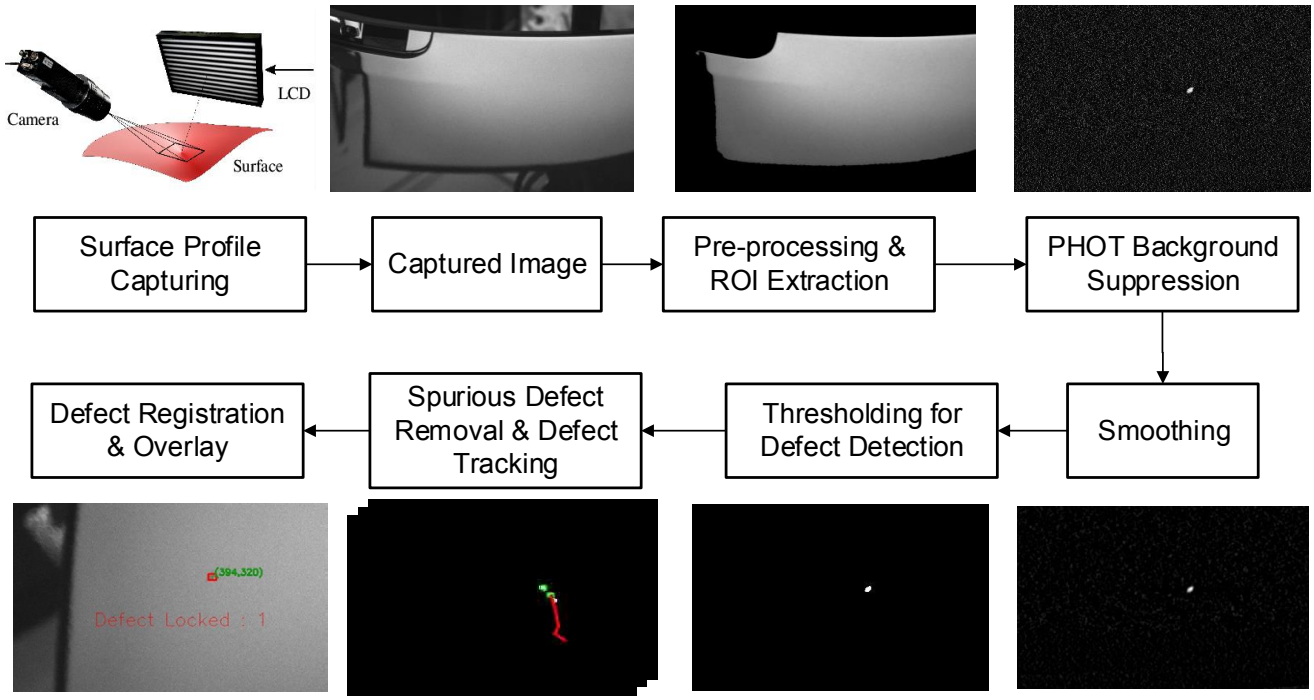

Fig. 1: Developed defect detection system and its key components

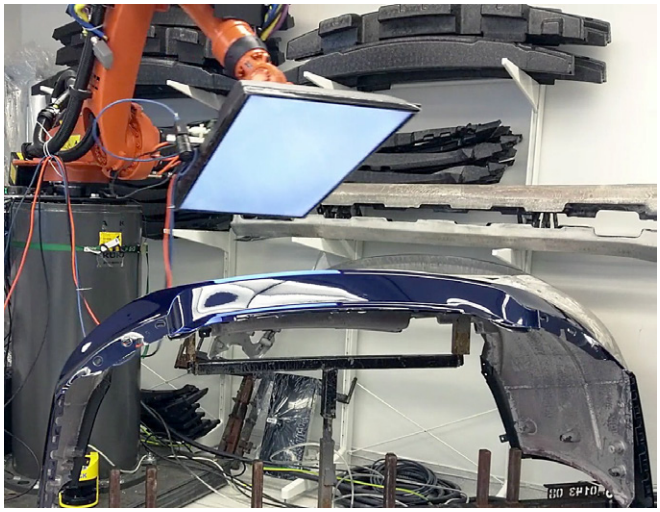

Fig. 2: Automatic defect detection set up

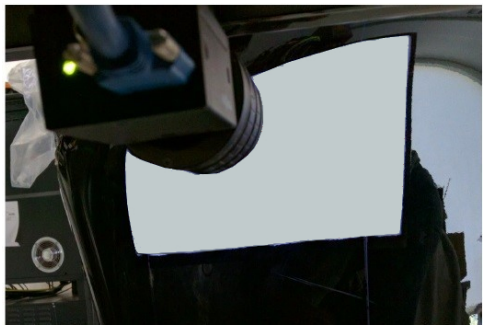

Fig. 3: Screen attached camera and its view

every pixel. This image is then thresholded to find the defect region. The threshold acts as the sensitivity parameter of the defect detection algorithm.

C. Spurious defect removal

The use of a single image can produce spurious defects as a result of any noise in the image. Since a continuous stream of images is available for defect detection, a true defect will appear in several consecutive frames. A Kalman filter assisted iterative hungarian algorithm is implemented for defect association and tracking to eliminate such spurious defects [34]. The implemented spurious defect elimination algorithm assigns a defect label only if a defect appears in a certain number of consecutive frames based on this data association. One such example showing true and spurious defects in consecutive video frames (Frame#174-183) is shown in Fig. 4, where true defects are represented by trailing coloured lines.

D. Defect feature extraction and registration

Once spurious defects are removed from the defect bank, defect attributes such as area, perimeter, centroid etc. are extracted. Nearby defects are clustered together, and then a contour-finding algorithm extracts these features. A database is used to record these defect statistics. Finally, the results are localized and overlaid on the part image for further assessment.

E. Administrative Control

A GUI, as shown in Fig. 5, is designed to provide different controls for this defect detection system. It has options to choose different fringe patterns, determine minimum detected defect size, select the segmentation type to segregate

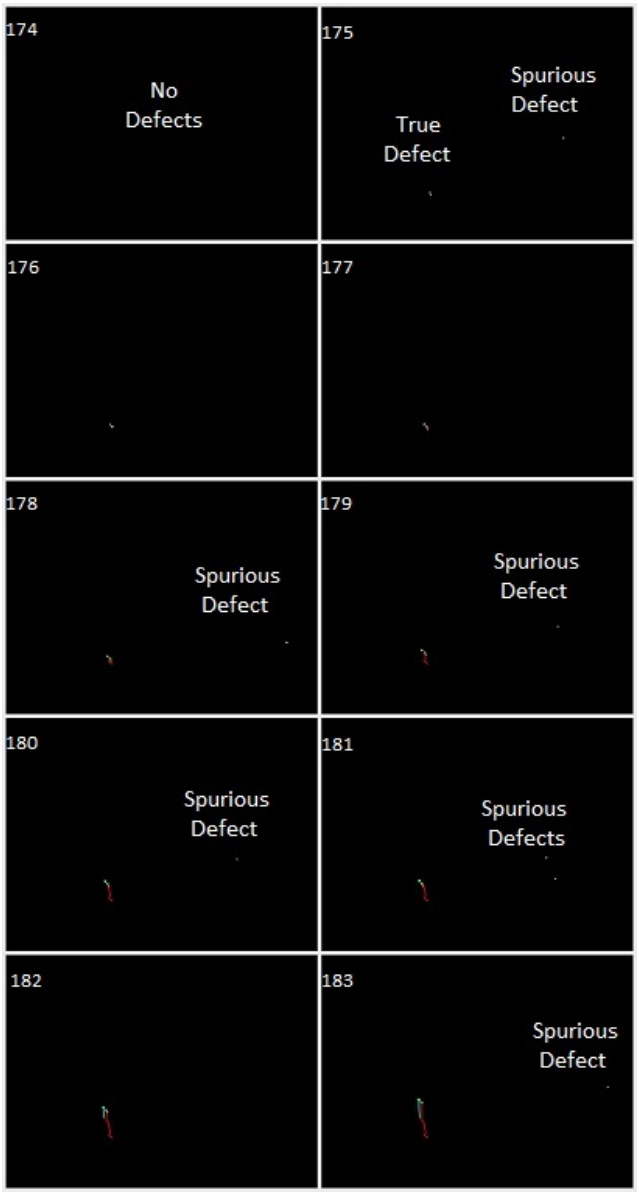

Fig. 4: Spurious defect elimination and defect tracking (Frame# 174-183). It can be seen that spurious defects are only present in a single frame and hence not tracked while true defects (in the bottom left corner) are present in continuous frames and are tracked as indicated by the trailing red and green lines.

the area of interest in the captured image, choose different defect detection algorithms, select images to display, and also the system's progress. The extracted defect information is overlaid on the part image.

IV. Experimental Testing and Results

A. Implementation and experimental set-up

The proposed defect detection system is implemented on Linux based PC. A monochrome Point Grey 3.2 MP (GS3-U3-32S4M-C) camera with a 12.5 mm Fujinon lens is used which can operate at 121 fps. To enable defect tracking

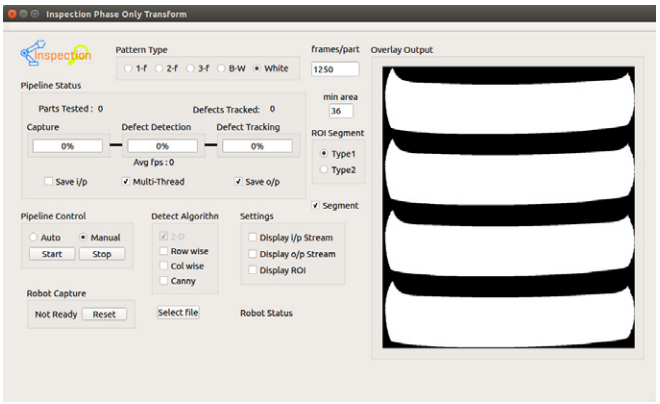

Fig. 5: Administrative control to select different attributes of defect detection system

and spurious defect elimination, the capture rate must be at least 90 fps capture rate. To achieve this rate, the captured image is reduced to 0.8 Mpixel (1024×768 pixels) before applying the defect detection algorithm. A 40 inch TV screen is used to display the pattern. For this testing, a solid white pattern is used. A Kuka industrial robot is used to scan the bumper surface and is operated at half of its maximum speed during lab testing due to safety reasons. The test bumper is mounted on an industrial carrier. Automobile bumpers used in this study are of different colours and are approximately 5.5 ft wide, 1.5 ft high and 2.5 ft deep (minivan bumpers). A distance of approximately 400 mm is maintained between the camera and test surface throughout the inspection process to keep the test surface in focus as a fixed focal length lens is used. As the camera starts capturing the images, the defect detection algorithm processes them in real-time. Once an anomaly is detected and tracked in a pre-defined number of consecutive frames, it is declared as a defect. The progress of these steps can be monitored on the provided administrative control GUI, shown in Fig. 5. With the given setup, the PHOT based defect detection system takes approximately 2 seconds to inspect half of a typical car bumper. This speed is within the manufacturing cycle time. This detection setup is depicted in Fig. 2.

B. System parameters

An extensive set of experiments were completed to determine the minimum frame rate, shutter speed and image size required for reliable defect detection and tracking. These results are summarized below:

- For spurious defect elimination and true defect tracking, multiple images of the same area are needed (although shifted due to robot movement), which requires a minimum 40 fps video stream.
- The algorithm works reliably on 0.8 Mpixel images and can detect larger than $0.5\ mm^2$ defects. The detection resolution can be altered by varying the image size or changing the distance between the camera and the test surface. This variation will affect the computation time as the PHOT-based analysis, which is the most computa-

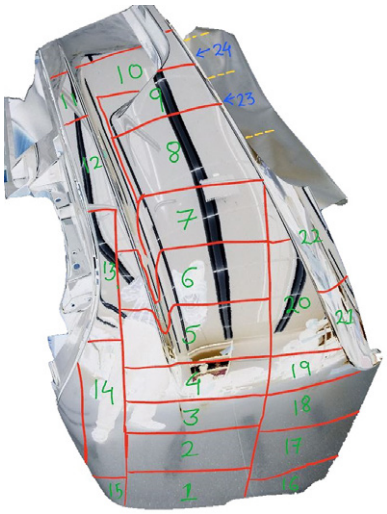

Fig. 6: Bumper segmentation for PSD-based defect detection. [16]©2018 IEEE

tionally expensive process in this detection framework, operates on the order of $O(nlogn)$.

- To minimize the motion blur introduced due to conveyor vibration and robot movement, camera shutter speed of 1-2 ms is used throughout testing.
- Defect detection algorithm works at 90 fps, which provides excellent defect tracking and spurious defect removal utilizing multi-threading.

C. Laboratory testing

The system was tested in two stages. The first stage involved lab verification and validation testing on a limited set of parts in a laboratory setting. Seven car bumpers parts were obtained from a local manufacturer. These parts were rejected due to various surface defects by human inspectors at the manufacturing facility. These defects are labelled ground truth (GT). The proposed system's performance is compared with a PSD-based system. PSD is a popular method for surface defect detection [9]–[18] and is used in the automotive industry for planer surface inspection. The version of PSD implemented is the one used in [16] where 7-phase shifted patterns are generated, and their reflection is captured, and the phase variations is used for surface reconstruction and defect detection. To capture 7-images for PSD, the robot divides the part into segments as it is impossible to inspect the whole bumper in one go due to its large size. This is illustrated in Fig. 6 where segments are annotated. During an inspection, the robot moves to each segment and then stops to capture the seven images before moving to the next one. This adds a significant delay to the inspection process.

Table I compares the results of the two methods on the ground truth (GT) data.

Based on the results in Table I, we calculated the precision, recall, and F-measure of every tested part according to the following equations. Results are provided in Table II. In some applications, FP (rejecting a good sample) is more forgivable than FN (missing defective region or sample), so different weights are applied to precision and recall.

TABLE I: Defect detection results

			Proposed system			PSD based system		
Part#	Color	GT	TP	FP	FN	TP	FP	FN
1	Black	17	11	0	6	9	1	8
2	Dark Blue	19	14	0	5	2	0	17
3	Dark Blue	5	4	0	1	2	1	3
4	Dark Silver	14	9	2	5	12	3	2
5	Dark Blue	3	2	0	1	1	3	2
6	Purple	7	7	3	0	2	1	5
7	Dark Silver	4	3	1	1	0	0	4
Aggregate		69	50	6	19	28	9	41

GT is ground truth, TP is true positive, FP is false positive and FN is false negative.

$$Precision = \frac{TP}{TP + FP} \tag{6}$$

$$Recall = \frac{TP}{TP + FN} \tag{7}$$

$$F - measure = 2 \times \frac{Precision \times Recall}{Precision + Recall} \tag{8}$$

TABLE II: Analysis of detection results for both techniques

	Proposed system			PSD based system		
Part#	Precision	Recall	F-meas	Precision	Recall	F-meas
1	1.00	0.65	0.79	0.90	0.53	0.67
2	1.00	0.74	0.85	1.00	0.11	0.19
3	1.00	0.80	0.89	0.67	0.40	0.50
4	0.82	0.64	0.72	0.80	0.86	0.83
5	1.00	0.67	0.80	0.25	0.33	0.29
6	0.70	1.00	0.82	0.67	0.29	0.4
7	0.75	0.75	0.75	NaN	0.00	NaN
Avg.	0.90	0.75	0.80	0.76	0.36	0.48

The results show that the proposed system significantly outperforms the PSD based system using all measures of detection and almost on all parts. In some cases, the performance is significantly better (e.g part 2, 5-7). Regardless of detection accuracy, from a practical perspective, the PSD system cycle time is 0.35 sec per segment [16]. This time does not include movement time between segments so it is not dependent on arm speed. Arm speed is determined by operational constraints at production facilities. Overall, PSD based inspection of half bumper takes approximately 13 seconds, whereas the proposed system completes the same task in under 2 seconds.

D. On-site Testing

The second stage of the system testing was completed at the parts manufacturing facility where a larger number of parts were available for testing. This facility has a test booth equipped with robotic arms, conveyor and part carriage. This testing setup simulates an identical manufacturing environment in terms of cycle time, parts configuration, and parts movement and vibration. The parts are mounted on a carriage (4 at a time), which moves on a conveyor. The inspection

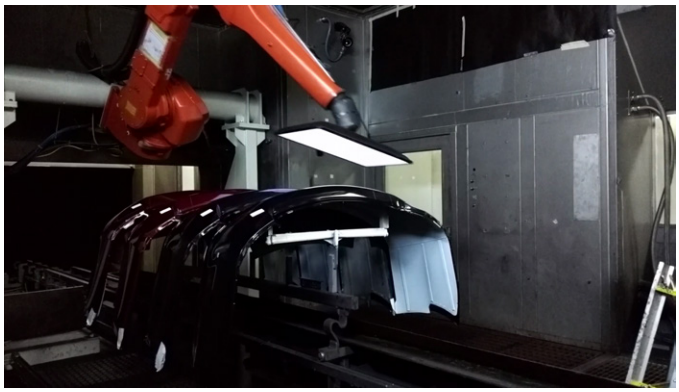

Fig. 7: Part inspection setup in test booth

process starts as the carriage arrives, the robot traversing and camera capture are synchronized with the part arrival on the conveyor system. The setup is shown in Fig. 7.

A total of 66-parts with different defects were inspected. All but one of these parts had different surface defects and hence were rejected. These defects are manually identified by human inspectors and were considered GT. A total of 183 defects are marked on the 66 inspected parts. The developed system has detected 112 TP, 38 FP and 71 FN, which results in a precision measure of 0.80 and a recall measure of 0.66. Some of these detection results are depicted in Fig. 8.

The precision and recall measures are slightly below that were observed during lab testing. To investigate why this was the case, we conducted a failure mode analysis. It was observed that approximately 80% of FP were the result of lint or dust particles that remained on the test part after the cleaning, which was performed to remove the GT markings. Most of the FN (about 65%) are the result of improper focus. Since, a fixed focal lens was used in this testing, variations in distance between the camera and test part due to part curvature may induce this issue. A lens with a greater depth of field (DoF) can reduce this issue and hence the number of detected FN.

We changed the lens to one with an 8 mm focal length lens and its aperture was set to f/2.8. This improved the DoF. The same parts were again tested at the manufacturer's facility and special care and attention were taken to clean dirt and lint particles from the parts. An improve defect detection performance is observed with a precision measure of 0.83 and a recall measure of 0.71. The failure mode analysis indicated that most of the FPs are the result of lint or dirt particles that were present in the environment and have resettled on the parts. This will be less of an issue in real production as the inspection is performed right after painting, where a dust-free environment is maintained. Reasons for FN is a combination of defect invisibility in the registered image and segmentation of ROI. It should also be noted that the GT is provided by human inspectors whose judgement also varies due to the factors mentioned earlier and, as a result, can diminish the performance of the developed system due to missed or wrongly identified defects.

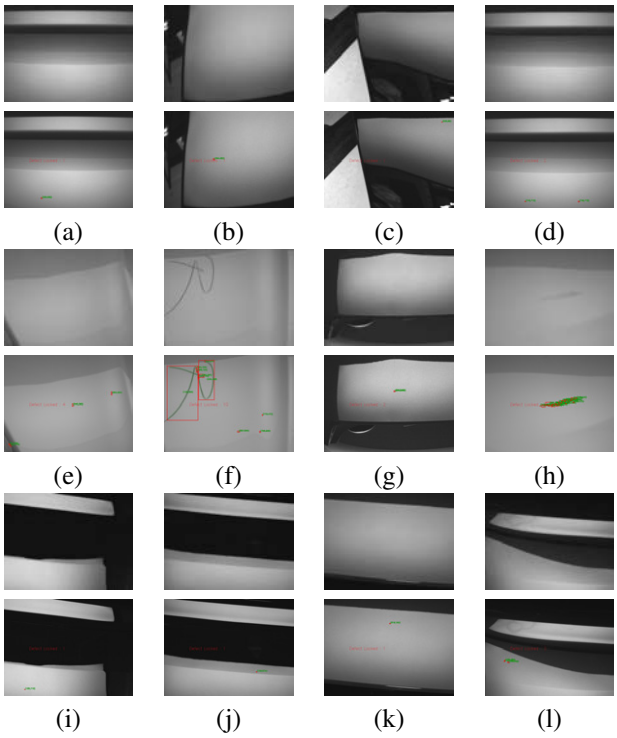

Fig. 8: Captured surface reflections (1st row) and corresponding defects deteted by the developed system (2nd row).

The system can detect defects larger than $0.5\ mm^2$ size. The sensitivity can be altered by changing the camera resolution or the distance between the test surface and camera. At present, a 0.8 Mpixel image is used, and a distance of 400 mm is maintained. A larger image can increase the sensitivity at the expense of greater computation overhead.

V. Conclusion

In this paper, we presented a robust robotics system for defect detection on semi-specular automotive surfaces. The system was tested in the lab and also on-site in a real manufacturing environment. The system can overcome significant operational challenges of part surface reflection, cycle time, part size, and part vibration to detect various defects with high precision. Several additional measures can improve accuracy. The removal of dirt and lint particles will improve precision by reducing FP. Having a more precise robot path planning will improve the FN occurring as a result of poor ROI and the invisibility of defects. A solid white pattern is used for the illumination of parts in this study, the effect of using multi-frequency pattern with varying grey level intensities can be investigated. The proposed system can also be used for the inspection of other semi-specular and specular surfaces of varied sizes and geometry such as metal sheets, liquid crystal displays (LCDs), and sphere parts. Finally we note that we compared results to human inspectors but human inspectors are not a reliable measure of ground truth. Deployment of the system will require a careful calibration stage to insure consistent performance.

REFERENCES

[1] Fernandez, C., Platero, C., Campoy, P., Aracil, R.: Vision system for on-line surface inspection in aluminum casting process. In: Proceedings of IECON '93 - 19th Annual Conference of IEEE Industrial Electronics. (Nov 1993) 1854–1859 vol.3

[2] Liu, Z., Wang, W., Zhang, X., Jia, W.: Inspection of rail surface defects based on image processing. CAR 2010 - 2010 2nd Int. Asia Conf. Informatics Control. Autom. Robot. **1** (2010) 472–475

[3] Liu, B., Wu, S., Zou, S.: Automatic detection technology of surface defects on plastic products based on machine vision. In: 2010 International Conference on Mechanic Automation and Control Engineering. (June 2010) 2213–2216

[4] Guo, J., Shao, W.: Automated detection of surface defects on sphere parts using laser and CDD measurements. IECON 2011 - 37th Annu. Conf. IEEE Ind. Electron. Soc. (2011) 2666–2671

[5] Janardhana, S., Jaya, J., Sabareesaan, K.J., George, J.: Computer aided inspection system for food products using machine vision — A review. 2013 Int. Conf. Curr. Trends Eng. Technol. (2013) 29–33

[6] Cho CS, Chung BM, P.M.: Development of real-time vision based fabric inspection system. IEEE Trans Ind Electron **52(4)**(4) (2005) 1073–9

[7] Faber, C., Olesch, E., Krobot, R., Häusler, G.: Deflectometry challenges interferometry - the competition gets tougher! Proceedings of SPIE - The International Society for Optical Engineering **8493** (09 2012)

[8] Ritter, R., Hahn, R.: Contribution to analysis of the reflection grating method. Opt Lasers Eng **4**(1) (1983) 13–24

[9] Armesto, L., Tornero, J., Herraez, A., Asensio, J.: Inspection system based on artificial vision for paint defects detection on cars bodies. In: 2011 IEEE International Conference on Robotics and Automation. (May 2011) 1–4

[10] Takeda, M., Ina, H., Kobayashi, S.: Fourier-transform method of fringe-pattern analysis for computer-based topography and interferometry. J. Opt. Soc. Am. **72**(1) (1982) 156–160

[11] Tarry, C., Stachowsky, M., Moussa, M.: Robust detection of paint defects in moulded plastic parts. Proc. - Conf. Comput. Robot Vision, CRV 2014 (2014) 306–312

[12] Puente León, F., Kammel, S.: Inspection of specular and painted surfaces with centralized fusion techniques. Meas. J. Int. Meas. Confed. **39** (2006) 536–546

[13] Surrel, Y.: Deflectometry: A simple and efficient noninterferometric method for slope measurement. Xth SEM Int. Congr. Exp. Mech. (2004)

[14] Caulier, Y.: Inspection of complex surfaces by means of structured light patterns. Opt. Express **18**(7) (Mar 2010) 6642–6660

[15] Peng, X., Chen, Y., Yu, W., Zhou, Z., Sun, G.: An online defects inspection method for float glass fabrication based on machine vision. The International Journal of Advanced Manufacturing Technology **39** (12 2008) 1180–1189

[16] Tandiya, A., Akthar, S., Moussa, M., Tarray, C.: Automotive semi-specular surface defect detection system. In: 2018 15th Conference on Computer and Robot Vision (CRV). (May 2018) 285–291

[17] Molina, J., Solanes, J.E., Arnal, L., Tornero, J.: On the detection of defects on specular car body surfaces. Robotics and Computer-Integrated Manufacturing **48** (2017) 263 – 278

[18] Akhtar, S., Tandiya, A., Moussa, M., Tarry, C.: An Efficient Automotive Paint Defect Detection System. Advances in Science, Technology and Engineering Systems Journal **4**(3) (2019) 171–182

[19] Wei Fan, Lu, C., Tsujino, K.: An automatic machine vision method for the flaw detection on car's body. In: 2015 IEEE 7th International Conference on Awareness Science and Technology (iCAST). (Sep. 2015) 13–18

[20] Zhou, Q., Chen, R., Bin, H., Liu, C., Yu, J., Yu, X.: An automatic surface defect inspection system for automobiles using machine vision methods. Sensors **19** (02 2019) 644

[21] Schlegl, T., Seeböck, P., Waldstein, S.M., Schmidt-Erfurth, U., Langs, G.: Unsupervised anomaly detection with generative adversarial networks to guide marker discovery. In: Information Processing in Medical Imaging - 25th International Conference, IPMI 2017, Boone, NC, USA, June 25-30, 2017, Proceedings. (2017) 146–157

[22] Kadurin, A., Nikolenko, S., Khrabrov, K., Aliper, A., Zhavoronkov, A.: drugan: An advanced generative adversarial autoencoder model for de novo generation of new molecules with desired molecular properties in silico. Molecular Pharmaceutics **14**(9) (2017) 3098–3104 PMID: 28703000.

[23] Cong, Y., Yuan, J., Liu, J.: Sparse reconstruction cost for abnormal event detection. In: CVPR 2011. (June 2011) 3449–3456

[24] Li, W., Mahadevan, V., Vasconcelos, N.: Anomaly detection and localization in crowded scenes. IEEE Trans. Pattern Anal. Mach. Intell. **36**(1) (January 2014) 18–32

[25] Sabokrou, M., Fayyaz, M., Fathy, M., Klette, R.: Deep-cascade: Cascading 3d deep neural networks for fast anomaly detection and localization in crowded scenes. IEEE Transactions on Image Processing **26**(4) (February 2017) 1992–2004

[26] Xia, Y., Cao, X., Wen, F., Hua, G., Sun, J.: Learning discriminative reconstructions for unsupervised outlier removal. In: 2015 IEEE International Conference on Computer Vision, ICCV 2015, Santiago, Chile, December 7-13, 2015. (2015) 1511–1519

[27] Markou, M., Singh, S.: Novelty detection: A review - part 1: Statistical approaches. Signal Processing **83**(12) (2003) 2481 – 2497

[28] Markou, M., Singh, S.: Novelty detection: A review - part 2: Neural network based approaches. Signal Processing **83**(12) (2003) 2499–2521

[29] Pimentel, M.A.F., Clifton, D.A., Clifton, L., Tarassenko, L.: Review: A review of novelty detection. Signal Process. **99** (June 2014) 215–249

[30] Aiger, D., Talbot, H.: The phase only transform for unsupervised surface defect detection. Proc. IEEE Comput. Soc. Conf. Comput. Vis. Pattern Recognit. (2010) 295–302

[31] Chan, C.H., Pang, G.K.H.: Fabric defect detection by Fourier analysis. Industry Applications, IEEE Transactions on **36**(5) (August 2002) 1267–1276

[32] Oppenheim, A.V., Lim, J.S.: The importance of phase in signals. IEEE Proceedings **69** (May 1981) 529–541

[33] Gonzalez, R.C., Woods, R.E.: Digital Image Processing (3rd Edition). Prentice-Hall, Inc., Upper Saddle River, NJ, USA (2006)

[34] Sahbani, B., Adiprawita, W.: Kalman filter and iterative-hungarian algorithm implementation for low complexity point tracking as part of fast multiple object tracking system. In: 2016 6th International Conference on System Engineering and Technology (ICSET). (Oct 2016) 109–115